AMERICAN SOCIETY FOR MICROBIOLOGY | Molecular and Cellular Biology®

RESEARCH ARTICLE

Transforming Growth Factor β-Induced Proliferative Arrest Mediated by TRIM26-Dependent TAF7 Degradation and Its Antagonism by MYC

Tadashi Nakagawa,[a] Masaki Hosogane,[a] Makiko Nakagawa,[a] Akane Morohoshi,[a] Ryo Funayama,[a] Keiko Nakayama[a]

[a]Division of Cell Proliferation, ART, Graduate School of Medicine, Tohoku University, Sendai, Miyagi, Japan

ABSTRACT Recognition of gene promoters by RNA polymerase II is mediated by general transcription factor IID (TFIID), which has been thought to be a static complex and to play a passive role in the regulation of gene expression under the instruction of gene-specific transcription factors. Here we show that transforming growth factor β (TGF-β) induced degradation of the TFIID subunit TAF7 in cultured mouse mammary epithelial cells and that this effect was required for proliferative arrest in response to TGF-β stimulation. TGF-β stimulated transcription of the gene for the ubiquitin ligase TRIM26, which was shown to ubiquitylate TAF7 and thereby to target it for proteasomal degradation. Sustained exposure of cells to TGF-β resulted in recovery from proliferative arrest in association with amplification of the *Myc* proto-oncogene, with MYC inhibiting TRIM26 induction by TGF-β. Our data thus show that TFIID is not simply a general mediator of transcription but contributes to the regulation of transcription in response to cell stimulation, playing a key role in the cytostatic function of TGF-β.

KEYWORDS MYC, TAF7, TGF-β, TRIM26, proliferation arrest, ubiquitylation

Transforming growth factor β (TGF-β) is a pleiotropic cytokine that activates SMAD transcription factors via a receptor serine-threonine kinase (1). TGF-β functions as a pro-oncogenic factor through induction of the epithelial-mesenchymal transition (EMT), which confers characteristics associated with cancer stem cells and malignancy in epithelial cells (2). On the other hand, TGF-β also has the ability to inhibit cell proliferation and to induce apoptosis in most cell types, including epithelial cells (3). TGF-β is thus thought to act as a tumor suppressor at early stages of tumorigenesis but to promote invasiveness and metastasis in more advanced tumor cells (4). However, the molecular mechanisms by which tumor cells evade the restraining effect of TGF-β on cell proliferation have remained unclear.

Eukaryotic transcription is initiated by recognition of a gene promoter by general transcription factor IID (TFIID), a complex of TATA box binding protein (TBP) and TBP-associated factors (TAFs) (5). Whereas TFIID has been thought to be a static complex and to play a passive role in the selection of genes for transcriptional activation (6), recent studies have suggested that the stoichiometry of TFIID subunits is not static but is instead regulated in a cell-type-specific manner. Such cell-type-specific TFIID complexes are now thought to be important for selective gene expression during lineage-specific cell differentiation (7). Although many of these studies have shown that the differential expression of TFIID components is regulated at the transcriptional level, the possible role of posttranscriptional regulation—particularly at the level of protein degradation—has remained largely uninvestigated.

The degradation of nuclear proteins is regulated in large part by the ubiquitin-proteasome pathway, in which proteins tagged with multiple ubiquitin molecules undergo proteasome-catalyzed degradation (8, 9). Protein ubiquitylation requires three

Received 19 August 2017 **Returned for modification** 12 September 2017 **Accepted** 27 November 2017

Accepted manuscript posted online 4 December 2017

Citation Nakagawa T, Hosogane M, Nakagawa M, Morohoshi A, Funayama R, Nakayama K. 2018. Transforming growth factor β-induced proliferative arrest mediated by TRIM26-dependent TAF7 degradation and its antagonism by MYC. Mol Cell Biol 38:e00449-17. https://doi.org/10.1128/MCB.00449-17.

Address correspondence to Keiko Nakayama, nakayak2@med.tohoku.ac.jp.

T.N. and M.H. contributed equally to this article.

enzymes: a ubiquitin-activating enzyme (E1), a ubiquitin-conjugating enzyme (E2), and a ubiquitin ligase (E3). The ubiquitin ligase determines the substrate specificity of the ubiquitylation reaction (10, 11). The degradation of TAF4a and TBP during the differentiation of embryonal carcinoma cells and myoblasts has been shown to be suppressed by a proteasome inhibitor (12). A novel ubiquitin ligase that targets TBP in myotubes was recently identified and was shown to regulate myotube differentiation together with the proteasome (13), raising the possibility that the ubiquitin-proteasome system regulates additional TFIID components in other cellular processes, such as EMT.

Myc is one of the most frequently amplified oncogenes (14). Overexpression of the MYC protein increases the expression of genes that promote cell proliferation and negatively regulates that of genes related to proliferation arrest (15, 16), with these effects together facilitating tumor formation. MYC has been proposed to regulate gene expression both globally (17, 18) and selectively (19, 20). Genome-wide analyses have shown that MYC represses the expression of as many genes as it activates (21, 22), indicating the importance of such repression by MYC. However, the molecular mechanisms by which MYC acts as a transcriptional repressor have remained largely uncharacterized. In addition, the functional relationship between MYC and TGF-β in tumorigenesis is still mostly unknown.

We have now investigated the role of TFIID in TGF-β action and provide evidence that TGF-β and MYC signaling pathways converge at the level of gene expression for the ubiquitin ligase TRIM26, with TGF-β-induced proliferative arrest being mediated by TRIM26-dependent degradation of TAF7 and this effect being antagonized by MYC.

RESULTS

TGF-β induces proteasomal degradation of TAF7. Changes in the expression of TFIID subunits have been shown to be important for cellular differentiation (7). We investigated whether expression of TFIID subunits is also regulated by TGF-β by using NMuMG mouse mammary epithelial cells (23). Immunoblot analysis revealed a marked TGF-β-induced decrease in the amount of TAF7, whereas the abundance of the other subunits examined remained largely unchanged (Fig. 1A). To determine the mechanism of TAF7 downregulation, we measured the amount of *Taf7* mRNA. Reverse transcription (RT) and quantitative PCR (qPCR) analysis showed that it was increased rather than decreased in response to TGF-β stimulation (Fig. 1B), suggesting that the change in the amount of TAF7 protein was mediated at the posttranscriptional level rather than at the transcriptional level. Given that the TFIID components TAF4a and TBP were previously found to be degraded by the proteasome during differentiation of F9 embryonal carcinoma cells and C2C12 myoblasts (12), we examined the effects of the proteasome inhibitor MG132 in our system. We found that MG132 attenuated TGF-β-induced TAF7 degradation in NMuMG cells (Fig. 1C), suggesting that TAF7 is degraded by the proteasome in response to TGF-β stimulation. Given that the abundance of TAF4a and TBP was not affected by TGF-β in NMuMG cells, proteasomal degradation of TFIID components may be cell type or stimulus specific.

TGF-β-induced binding of TRIM26 to TAF7. Given that most proteins that undergo degradation by the proteasome are ubiquitylated, we searched for a ubiquitin ligase that might mediate TAF7 ubiquitylation. On the basis of the observation that TAF7 degradation was first apparent $\sim$12 h after the onset of exposure of NMuMG cells to TGF-β (Fig. 2A), we hypothesized that the putative ubiquitin ligase for TAF7 is induced at the transcriptional level by TGF-β. Examination of genome-wide gene expression data for NMuMG cells treated with TGF-β for 2 days or not treated (24) revealed that transcription of the genes for six ubiquitin ligases (RNF19B, RNF157, SMURF1, TRIM12C, TRIM26, and TRIM34B) and four substrate adaptor proteins of cullin-type ubiquitin ligases (FBXL20, FBXO32, KLHL21, and KLHL26) was increased by TGF-β stimulation, with a change cutoff of $>$1.5-fold (Fig. 2B). Cullin-type ubiquitin ligases require neddylation for activation, and this process is inhibited by the small-molecule drug MLN4924 (25). The observation that MLN4924 inhibited TGF-β-induced

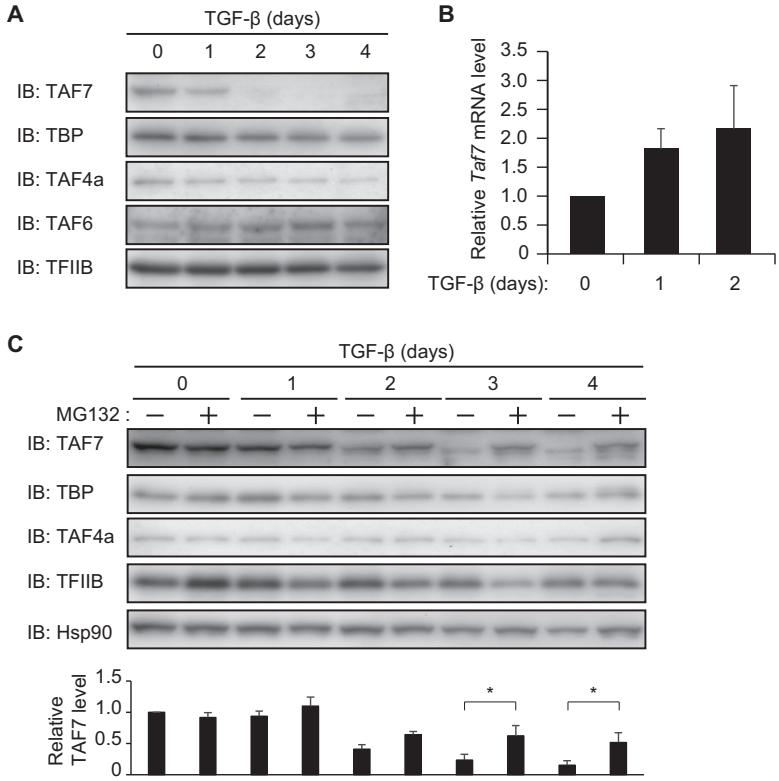

FIG 1 TAF7 is degraded by the proteasome in response to TGF-β stimulation in NMuMG cells. (A) Immunoblot (IB) analysis of TFIID subunits in NMuMG cells treated with TGF-β (4 ng/ml) for the indicated times. TFIIB served as a loading control. (B) The amounts of *Taf7* mRNA in NMuMG cells treated with TGF-β for the indicated times were determined by RT-qPCR analysis. Data are means and SEM for two independent experiments. (C) Immunoblot analysis of TFIID subunits in NMuMG cells treated with TGF-β for the indicated times and exposed (or not) to MG132 (10 μM) for 5 h before cell harvest. TFIIB and Hsp90 served as loading controls. The band intensities for TAF7 normalized to those for TFIIB are shown as means and SEM for three independent experiments. *, $P < 0.05$ (two-way ANOVA followed by Tukey's *post hoc* test).

degradation of the cullin substrate p27 but not that of TAF7 (Fig. 2C) suggested that a cullin-type ubiquitin ligase would not be responsible for TAF7 ubiquitylation.

Among the six remaining candidate ubiquitin ligases for TAF7, the amounts of the mRNAs for RNF19B, TRIM26, SMURF1, and RNF157 were increased after exposure of NMuMG cells to TGF-β for 24 h (Fig. 2D), at which time about half of TAF7 was already degraded (Fig. 2A). We examined whether TAF7 might interact with these four ubiquitin ligases and found that TRIM26, but not the other three enzymes, bound to TAF7 in transfected 293T cells (Fig. 2E to H). We also confirmed that TRIM26 directly bound to TAF7 *in vitro* (Fig. 2I). These data led us to focus on TRIM26 as a potential ubiquitin ligase for TAF7.

TRIM26 ubiquitylates TAF7 for proteasomal degradation. TRIM26 is a RING finger-type ubiquitin ligase in which the RING domain is necessary for catalysis of protein ubiquitylation. Overexpression of TRIM26 increased the level of TAF7 ubiquitylation in transfected 293T cells, whereas forced expression of a TRIM26 mutant lacking the RING domain (ΔRING) did not (Fig. 3A), indicating that the ubiquitin ligase activity of TRIM26 is required for TAF7 ubiquitylation. We also found that TRIM26 mediated the ubiquitylation of TAF7 *in vitro*, in an E1- and E2 (UBCH5A to -C)-dependent manner (Fig. 3B and C). We also confirmed that these E2 enzymes directly bound to TRIM26 (Fig. 3D). These data thus supported the notion that TRIM26 is a ubiquitin ligase for TAF7.

To investigate whether TRIM26 is required for TAF7 ubiquitylation and subsequent degradation in response to TGF-β treatment, we generated TRIM26-deficient NMuMG cells by use of the clustered regularly interspaced short palindromic repeat (CRISPR)-

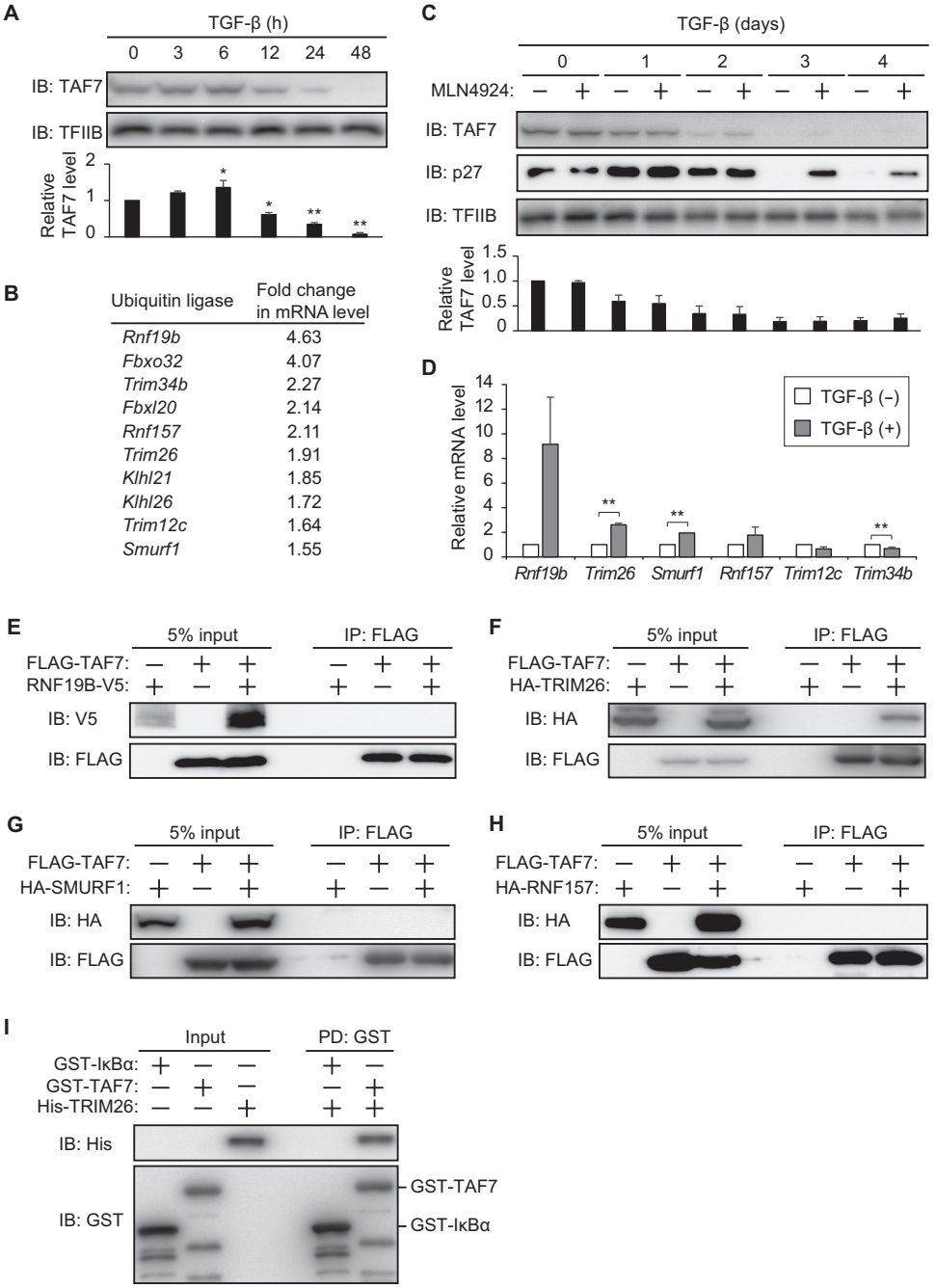

FIG 2 The TGF-β-induced ubiquitin ligase TRIM26 binds to TAF7. (A) Immunoblot analysis of TAF7 and TFIIB (loading control) in NMuMG cells treated with TGF-β for the indicated times. The band intensities for TAF7 normalized to those for TFIIB are shown as means and SEM for three independent experiments. *, $P < 0.05$; **, $P < 0.01$ versus 0 h (one-way ANOVA followed by Tukey's *post hoc* test). (B) Fold changes in abundance of mRNAs for the indicated ubiquitin ligases or substrate adaptor subunits for cullin-type ubiquitin ligases in NMuMG cells treated with TGF-β for 2 days relative to that in nontreated cells. Data are derived from a previously described microarray analysis (24). (C) Immunoblot analysis of TAF7, p27, and TFIIB (loading control) in NMuMG cells treated with TGF-β for the indicated times and exposed (or not) to MLN4924 (1 μM) for 5 h before cell harvest. The band intensities for TAF7 normalized to those for TFIIB are shown as means and SEM for three independent experiments. (D) RT-qPCR analysis of the indicated ubiquitin ligase mRNAs in NMuMG cells incubated in the absence or presence of TGF-β for 1 day. Data are means and SEM for three independent experiments. **, $P < 0.01$ (unpaired Student's *t* test). (E to H) Analysis of the binding of FLAG-tagged TAF7 to V5-tagged RNF19B (E), hemagglutinin (HA)-tagged TRIM26 (F), HA-tagged SMURF1 (G), or HA-tagged RNF157 (H) in transfected 293T cells. Cells transfected with expression plasmids encoding these proteins were subjected to immunoprecipitation (IP) with antibodies to FLAG. The resulting precipitates as well as the original cell lysates (5% input) were subjected to immunoblot analysis with antibodies to V5 or HA and FLAG. (I) Analysis of the binding of glutathione *S*-transferase (GST)-tagged TAF7 or GST-IκBα (negative control) to His_6-tagged TRIM26 *in vitro*. The recombinant proteins were expressed in and

(Continued on next page)

Cas9 system to disrupt the *Trim26* gene (Fig. 3E and F) and found that the prevention of TRIM26 induction in these cells was associated with attenuation of TGF-β-induced TAF7 degradation (Fig. 3G). Together these findings show that TRIM26 is a TGF-β-inducible ubiquitin ligase that ubiquitylates TAF7 for proteasomal degradation.

***Trim26* is a direct target of SMAD3.** We next examined the mechanism of TRIM26 induction by TGF-β. The TGF-β-induced increase in the abundance of *Trim26* mRNA in NMuMG cells was first apparent at 3 h (Fig. 4A) and was followed by protein induction at 6 h (Fig. 4B), indicating that *Trim26* is an immediate response gene. Note that TRIM26 induction occurred before TAF7 degradation, consistent with the notion that TRIM26 ubiquitylates TAF7 for degradation. The binding of TGF-β to its cell surface receptors results in the phosphorylation of receptor-regulated SMAD proteins (SMAD2 and SMAD3) and their consequent association with SMAD4 and translocation to the nucleus, where they form an active transcriptional complex that regulates the expression of target genes (1). Given that many SMAD target genes contain a SMAD binding element (SBE) in their promoter regions (26), we analyzed the mouse genome and identified two SBEs, at positions ~300 bp upstream (SBE1) and downstream (SBE2) of the transcription start site of *Trim26* (Fig. 4C). Chromatin immunoprecipitation (ChIP) followed by qPCR analysis revealed that TGF-β treatment resulted in an increase in the association of SMAD3 with SBE1 and SBE2 of *Trim26* in NMuMG cells (Fig. 4D). The specificity of this experiment was confirmed by loss of ChIP-qPCR signals in NMuMG cells depleted of SMAD3 by infection with retroviruses encoding specific short hairpin RNAs (shRNAs) (Fig. 4E and F). A luciferase reporter assay showed that the *Trim26* promoter was activated by TGF-β and that such activation was not observed with a promoter construct lacking both SBEs (ΔSBE1+ΔSBE2) (Fig. 4G). On the basis of these results, we concluded that *Trim26* is a direct target of SMAD3 activated by TGF-β.

TRIM26 induction and TAF7 degradation are important for TGF-β-induced proliferative arrest and apoptosis. Deletion of the *Taf7* gene in mouse embryonic fibroblasts was previously shown to induce proliferation arrest and cell death (27), effects that are also induced by TGF-β. To investigate the contribution of TRIM26-dependent TAF7 degradation to these actions of TGF-β, we examined the effects of TGF-β on cell proliferation and apoptosis in NMuMG cells depleted (or not) of TRIM26. We found that knockout of *Trim26* attenuated both TGF-β-induced proliferative arrest, as revealed by measurement of bromodeoxyuridine (BrdU) incorporation (Fig. 5A), and TGF-β-induced apoptosis, as revealed by flow cytometric analysis of cells stained with propidium iodide (PI) and annexin V (Fig. 6A). Furthermore, small interfering RNA (siRNA)-mediated depletion of TAF7 (Fig. 5B and C and 6B) or forced expression of enhanced green fluorescent protein (EGFP)-tagged TRIM26 (Fig. 5D and E and 6C) induced proliferative arrest and apoptosis even in the absence of TGF-β, whereas expression of FLAG epitope-tagged TAF7 suppressed TGF-β-induced proliferative arrest and apoptosis (Fig. 5F and G and 6D). In addition, siRNA-mediated depletion of TAF7 in *Trim26* knockout cells induced proliferative arrest as well as attenuating the resistance of these cells to TGF-β-induced proliferative arrest (data not shown). These results thus suggested that TGF-β-induced proliferation arrest and apoptosis are mediated, at least in part, by TRIM26 induction and subsequent TAF7 degradation.

In addition to proliferative arrest and apoptosis, TGF-β also induces EMT in NMuMG cells (23). We monitored this process by analysis of marker gene expression, with TGF-β downregulating the abundance of E-cadherin mRNA, a marker of epithelial cells, and upregulating that of N-cadherin mRNA, a mesenchymal marker (Fig. 7A). We also confirmed that the amounts of *Pai1* and *Snail* mRNAs, additional markers of EMT, were increased by TGF-β exposure (Fig. 7A). However, siRNA-mediated TAF7 depletion did

FIG 2 Legend (Continued)
purified from bacteria and then incubated in the indicated combinations for 60 min at 4°C. The GST-tagged proteins were precipitated with glutathione-agarose beads, and the resulting precipitates (PD) as well as the original binding mixtures (5% for His_6-TRIM26 and 50% for GST-tagged proteins) were subjected to immunoblot analysis with antibodies to His_6 and GST.

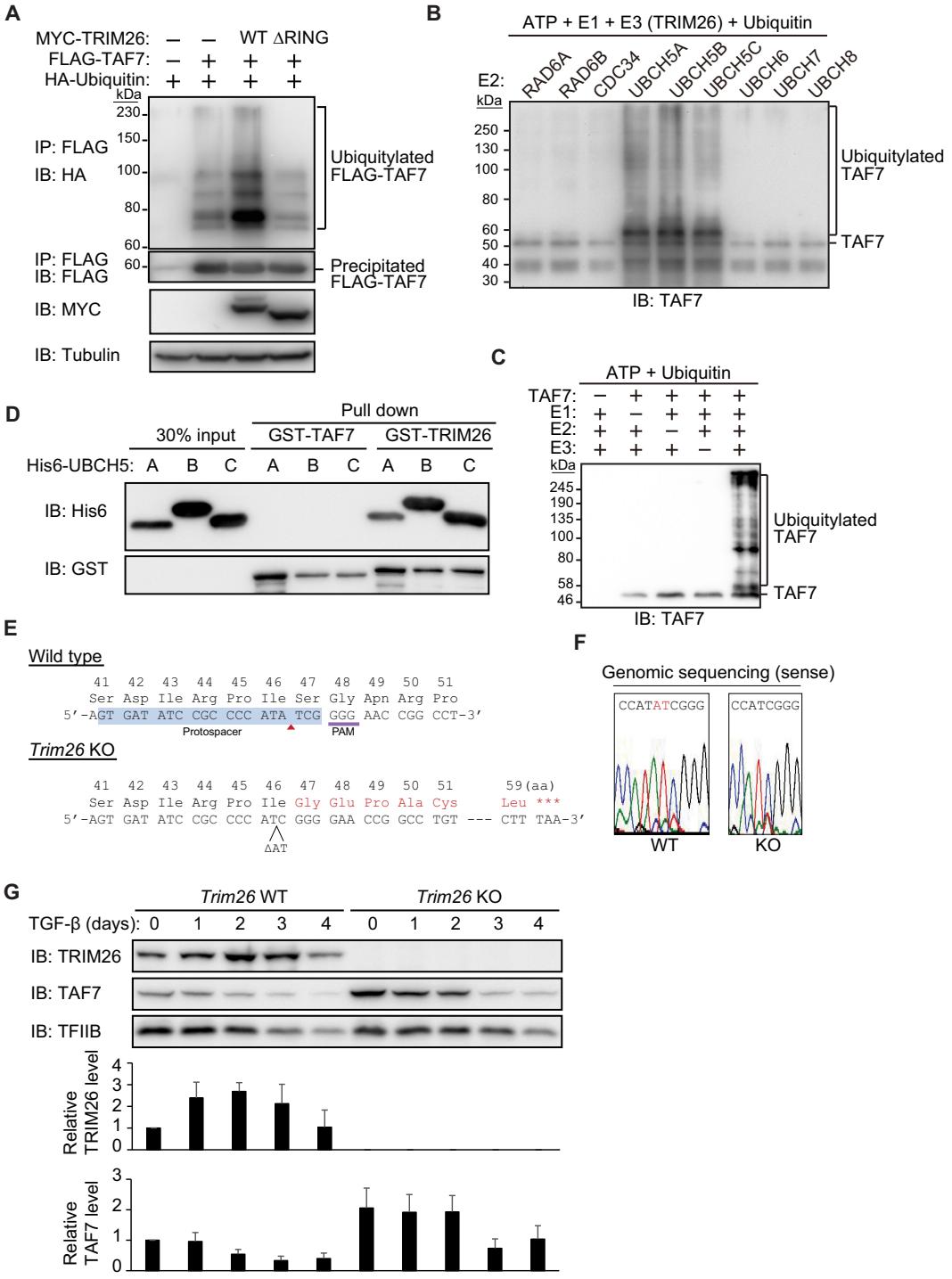

FIG 3 TRIM26 ubiquitylates TAF7 for proteasomal degradation. (A) Analysis of TAF7 ubiquitylation in transfected 293T cells. Cells transfected with the indicated combinations of expression plasmids for FLAG epitope-tagged TAF7, MYC epitope-tagged TRIM26 (wild type [WT] or a mutant lacking the RING domain [ΔRING]), and HA-tagged ubiquitin were treated for 5 h with MG132 (10 μM) and then subjected to immunoprecipitation with antibodies to FLAG under denaturing conditions. The resulting precipitates were subjected to immunoblot analysis with antibodies to HA and FLAG, and the original cell lysates were subjected to immunoblot analysis with antibodies to the MYC tag and α-tubulin (loading control). (B) Analysis of TAF7 ubiquitylation with various E2 enzymes *in vitro*. Reactions were performed for 120 min with ATP, ubiquitin, TAF7, E1, E3 (TRIM26), and the indicated E2 enzymes, after which reaction mixtures were subjected to immunoblot analysis with antibodies to TAF7. (C) Analysis of TAF7 ubiquitylation *in vitro*. Reactions were performed for 120 min with ATP, ubiquitin, and the indicated combinations of TAF7, E1, E2 (UBCH5A), and E3 (TRIM26), after which reaction mixtures were subjected to immunoblot analysis with antibodies to TAF7. (D) The binding of GST-tagged TRIM26 or GST-TAF7 (negative control) to the indicated His_6-tagged E2 enzymes *in vitro* was examined as described in the legend to Fig. 2I. (E) Strategy for mutagenesis of mouse *Trim26* by use of the CRISPR-Cas9 system. The protospacer sequence is highlighted, the protospacer-adjacent motif

(Continued on next page)

not induce substantial changes in EMT-related gene expression (Fig. 7B), indicating that TRIM26-dependent TAF7 degradation does not contribute to EMT progression.

Resumption of cell proliferation is associated with *Myc* amplification after sustained TGF-β treatment. NMuMG cells subjected to sustained exposure to TGF-β eventually resume proliferation with the mesenchyme-like phenotype intact (28). Given that TRIM26-mediated downregulation of TAF7 was associated with proliferation arrest in TGF-β-treated NMuMG cells, we examined whether TRIM26 induction was abrogated when the cells resumed proliferation. We treated NMuMG cells with TGF-β for up to 28 days and confirmed that proliferation arrest was transient, with resumption of cell proliferation being apparent at ~10 days (Fig. 8A), without a change in the mesenchyme-like phenotype (data not shown). The expression of TRIM26 mRNA and protein was upregulated at 7 days, when the cells had ceased proliferation, but was downregulated at 24 days, when the cells had resumed proliferation (Fig. 8B and C). Conversely, the amount of TAF7 protein was reduced at 7 days but had recovered at 24 days (Fig. 8C).

To investigate the molecular basis for the suppression of *Trim26* expression observed during persistent TGF-β exposure, we performed RNA sequencing (RNA-seq) analysis of cells exposed to TGF-β for 0, 7, or 28 days. We detected a marked increase in the expression of four genes—*Myc*, *Pvt1*, *Kif21a*, and *Abcd2*—28 days after the onset of exposure to TGF-β (Fig. 8D). Given that *Myc* and *Pvt1* as well as *Kif21a* and *Abcd2* are positioned side by side on chromosome 15, we reasoned that genomic amplification was likely responsible for the pronounced increases in transcript abundance. To verify this notion, we performed genomic DNA sequencing in order to determine the genome-wide DNA content for the cells treated with TGF-β for 0 or 28 days. Only two genomic regions, the *Myc/Pvt1* and *Kif21a/Abcd2* loci, were found to be amplified markedly in the cells exposed to TGF-β for 28 days (Fig. 8E and data not shown). Among these four genes, we focused on *Myc* because the human gene is frequently amplified in breast cancer (29). We validated the overexpression of *Myc* by RT-qPCR analysis (Fig. 8F) and the genomic amplification around the *Myc/Pvt1* and *Kif21a/Abcd2* loci by genomic PCR analysis (Fig. 8G and data not shown) for two independent batches of NMuMG cells subjected to long-term TGF-β treatment. The data thus suggested that *Myc* overexpression caused by genomic amplification might trigger the resumption of proliferation in cells subjected to persistent exposure to TGF-β. The NMuMG cells with acquired resistance to TGF-β-induced proliferative arrest were designated rNMuMG cells for further analysis.

rNMuMG cells are resistant to *Trim26* induction by TGF-β. To investigate whether rNMuMG cells had lost the ability to respond to TGF-β, we cultured them for 7 days without TGF-β and then reexposed them to the cytokine. TGF-β reexposure did not trigger TRIM26 protein induction or TAF7 degradation (Fig. 9A), nor did it induce proliferation arrest or a substantial level of apoptosis (data not shown). RT-qPCR analysis also revealed that the abundance of *Trim26* mRNA was not increased by reexposure of rNMuMG cells to TGF-β (Fig. 9B). However, E-cadherin mRNA was downregulated and both N-cadherin and *Snail* mRNAs were upregulated by TGF-β in rNMuMG cells, to extents similar to those apparent in the parental NMuMG cells (Fig. 9B), indicating that rNMuMG cells were able to respond to TGF-β but failed to induce TRIM26. To explore the mechanism underlying this failure of TRIM26 induction by TGF-β in rNMuMG cells, we focused on the overexpression of MYC, given that (i) such overexpression was apparent with or without TGF-β (Fig. 8D and 9A), (ii) there is an

FIG 3 Legend (Continued)
(PAM) is underlined, and the cleavage site is indicated by a red arrowhead. *Trim26* knockout (KO) NMuMG cells harbor a 2-nucleotide deletion in both alleles of *Trim26* that generates a codon frameshift after position 46 and results in truncation at position 59. (F) Sanger genomic sequencing results for WT (parental) and *Trim26* KO NMuMG cells showing the region of *Trim26* targeted by the CRISPR-Cas9 system. (G) Immunoblot analysis of TRIM26, TAF7, and TFIIB (loading control) in parental and *Trim26* KO NMuMG cells treated with TGF-β for the indicated times. The band intensities for TRIM26 and TAF7 normalized to those for TFIIB are shown as means and SEM for three independent experiments.

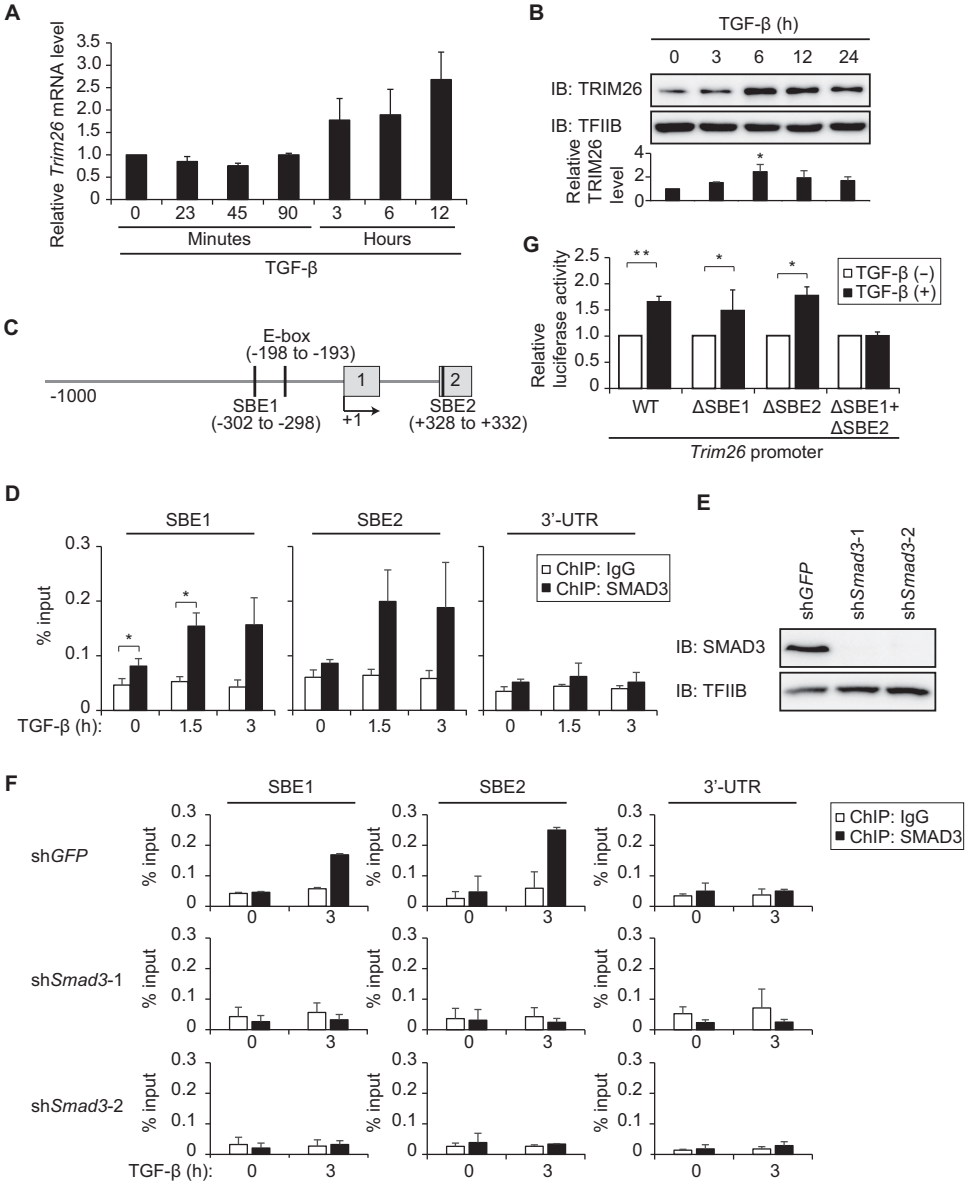

FIG 4 *Trim26* is a direct target of SMAD3. (A) RT-qPCR analysis of *Trim26* mRNA in NMuMG cells treated with TGF-β for the indicated times. Data are means and SEM for two independent experiments. (B) Immunoblot analysis of TRIM26 and TFIIB (loading control) in NMuMG cells treated with TGF-β for the indicated times. The band intensities for TRIM26 normalized to those for TFIIB are shown as means and SEM for three independent experiments. *, $P < 0.05$ versus 0 h (one-way ANOVA followed by Tukey's *post hoc* test). (C) Schematic representation of the mouse *Trim26* promoter region, showing putative SMAD binding elements (SBEs) and an E-box. The transcription start site is indicated as position +1, and numbered boxes denote exons. (D) ChIP-qPCR analysis of SMAD3 binding to the *Trim26* promoter region. NMuMG cells exposed to TGF-β for the indicated times were fixed, lysed, and subjected to ultrasonic treatment followed by ChIP with either antibodies to SMAD3 or control immunoglobulin G (IgG). Precipitated DNA was quantified by qPCR with primers specific for the indicated regions of *Trim26* (UTR, untranslated region). Data are means and SEM for three independent experiments. *, $P < 0.05$ (two-way ANOVA followed by Tukey's *post hoc* test). (E) Immunoblot analysis of SMAD3 and TFIIB (loading control) in NMuMG cells stably infected with retroviruses encoding shRNAs specific for *Smad3* or green fluorescent protein (*GFP*; control) mRNA. (F) ChIP-qPCR analysis of SMAD3 binding to the *Trim26* promoter region in NMuMG cells stably infected with retroviruses as described for panel E and exposed to TGF-β for 0 or 3 h. Data are means and SEM for two independent experiments. (G) Luciferase reporter assay of *Trim26* promoter activity. NMuMG cells were transfected with a luciferase reporter plasmid containing WT or SBE deletion mutant forms of the *Trim26* promoter (nucleotides −421 to +427) as well as with the pRL-CMV control plasmid. The cells were then treated with TGF-β for 24 h before assay of luciferase activities. Data are means and SEM for three independent experiments. *, $P < 0.05$; **, $P < 0.01$ (unpaired Student's *t* test).

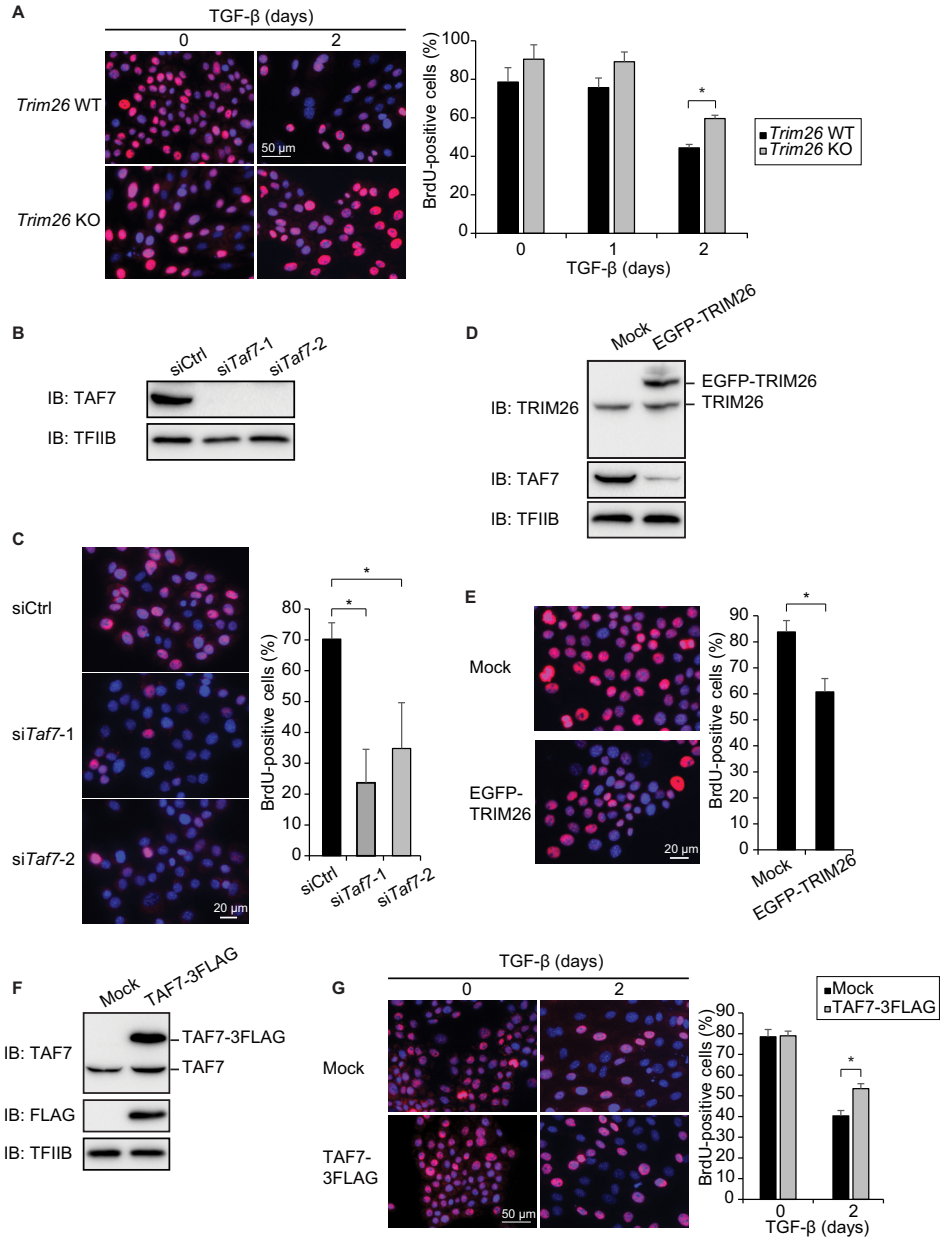

FIG 5 Downregulation of TAF7 is important for TGF-β-induced proliferation arrest. (A) (Left) Immunofluorescence staining of BrdU incorporation (red fluorescence) in parental (*Trim26* WT) or *Trim26* KO NMuMG cells incubated in the absence or presence of TGF-β for 2 days. Nuclei were stained with DAPI (blue fluorescence). (Right) The percentage of BrdU-positive cells was determined for each condition. Data are means and SEM for three independent experiments. *, $P < 0.05$ (two-way ANOVA followed by Tukey's *post hoc* test). (B) Immunoblot analysis of TAF7 and TFIIB (loading control) in NMuMG cells transfected with either of two siRNAs targeting *Taf7* mRNA or with a negative-control siRNA (siCtrl). (C) (Left) Immunofluorescence staining of BrdU incorporation (red fluorescence) in NMuMG cells transfected as described for panel B. Nuclei were stained with DAPI (blue fluorescence). (Right) The percentage of BrdU-positive cells was determined for each condition. Data are means and SEM for three independent experiments. *, $P < 0.05$ (one-way ANOVA followed by Tukey's *post hoc* test). (D) Immunoblot analysis of TAF7, TRIM26, and TFIIB (loading control) in NMuMG cells stably infected with a retrovirus encoding EGFP-tagged TRIM26 or with the empty virus (mock). (E) (Left) Immunofluorescence staining of BrdU incorporation (red fluorescence) in NMuMG cells stably infected as described for panel D. Nuclei were stained with DAPI (blue fluorescence). (Right) The percentage of BrdU-positive cells was determined for each condition. Data are means and SEM for three independent experiments. *, $P < 0.05$ (unpaired Student's *t* test). (F) Immunoblot analysis of TAF7, FLAG, and TFIIB (loading control) in NMuMG cells stably infected with a retrovirus encoding 3×FLAG-tagged TAF7 or with the empty virus (mock). (G) (Left) Immunofluorescence staining of BrdU incorporation (red fluorescence) in NMuMG cells stably infected as described for panel F and incubated in the absence or presence of TGF-β for 2 days. Nuclei were stained with DAPI (blue fluorescence). (Right) The percentage of BrdU-positive cells was determined for each condition. Data are means and SEM for three independent experiments. *, $P < 0.05$ (two-way ANOVA followed by Tukey's *post hoc* test).

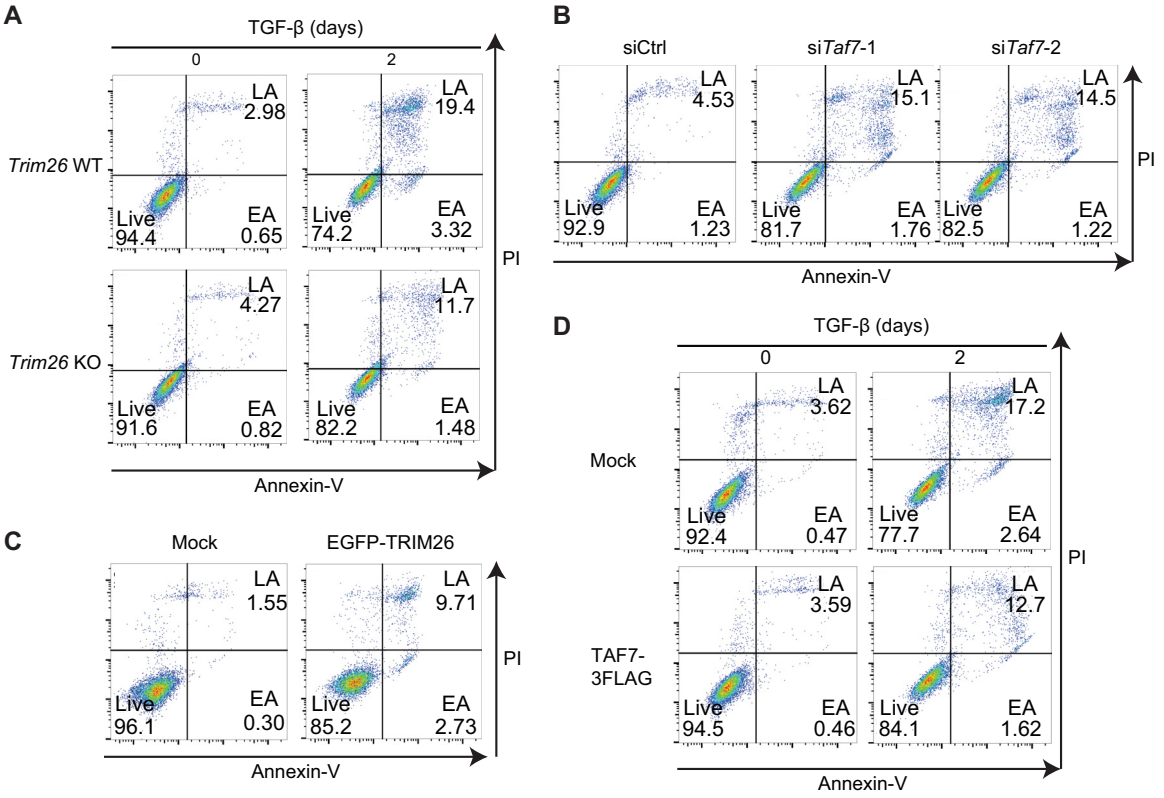

FIG 6 Downregulation of TAF7 is important for TGF-β-induced apoptosis. (A) Parental (*Trim26* WT) or *Trim26* KO NMuMG cells were incubated in the absence or presence of TGF-β for 2 days and then stained with PI and annexin V for flow cytometric analysis of apoptosis. EA, early apoptosis; LA, late apoptosis. (B) NMuMG cells transfected with either of two siRNAs targeting *Taf7* mRNA or with a negative-control siRNA (siCtrl) were stained with PI and annexin V for flow cytometric analysis of apoptosis. (C) NMuMG cells stably infected with a retrovirus encoding EGFP-tagged TRIM26 or with the empty virus (mock) were stained with PI and annexin V for flow cytometric analysis of apoptosis. (D) NMuMG cells stably infected with a retrovirus encoding 3×FLAG-tagged TAF7 or with the empty virus (mock) and incubated in the absence or presence of TGF-β for 2 days were stained with PI and annexin V for flow cytometric analysis of apoptosis.

E-box element (MYC binding site) in close proximity to SBE1 in the *Trim26* promoter (Fig. 4C), and (iii) MYC acts as a transcriptional repressor at a subset of its target genes (19, 20). ChIP-qPCR analysis of parental NMuMG cells revealed that MYC bound to the target region containing SBE1 (Fig. 9C), which also encompasses the E-box, suggesting that the E-box adjacent to SBE1 is functional. Furthermore, the increase in SMAD3 binding to SBE1 induced by TGF-β (Fig. 4D) was accompanied by loss of MYC from this genomic region (Fig. 9C). In rNMuMG cells treated with TGF-β, however, overexpressed MYC did not dissociate from the SBE1 region and SMAD3 was not recruited to SBE1 or SBE2 (Fig. 9D). Consistent with these data, the *Trim26* promoter was not activated by TGF-β in rNMuMG cells (Fig. 9E). Together these results suggested that overexpressed MYC impeded SMAD3 binding to SBE1 and consequent activation of the *Trim26* promoter. To provide further insight into the relationship between SMAD3 and MYC binding at the *Trim26* promoter, we depleted MYC in rNMuMG cells by siRNA transfection (data not shown) and found that such depletion resulted in recruitment of SMAD3 to SBE1 and SBE2 and that this effect was enhanced by TGF-β treatment (Fig. 9D). MYC depletion also led to a reduction in the extent of cell proliferation in rNMuMG cells exposed to TGF-β (data not shown). On the basis of these observations, we hypothesized that overexpressed MYC interferes with the binding of activated SMAD3 to the *Trim26* promoter and thereby inhibits TRIM26 induction and subsequent TAF7 degradation in rNMuMG cells.

Forced MYC overexpression suppresses TRIM26 induction by TGF-β. To test whether *Myc* overexpression alone is sufficient to suppress TRIM26 induction, we

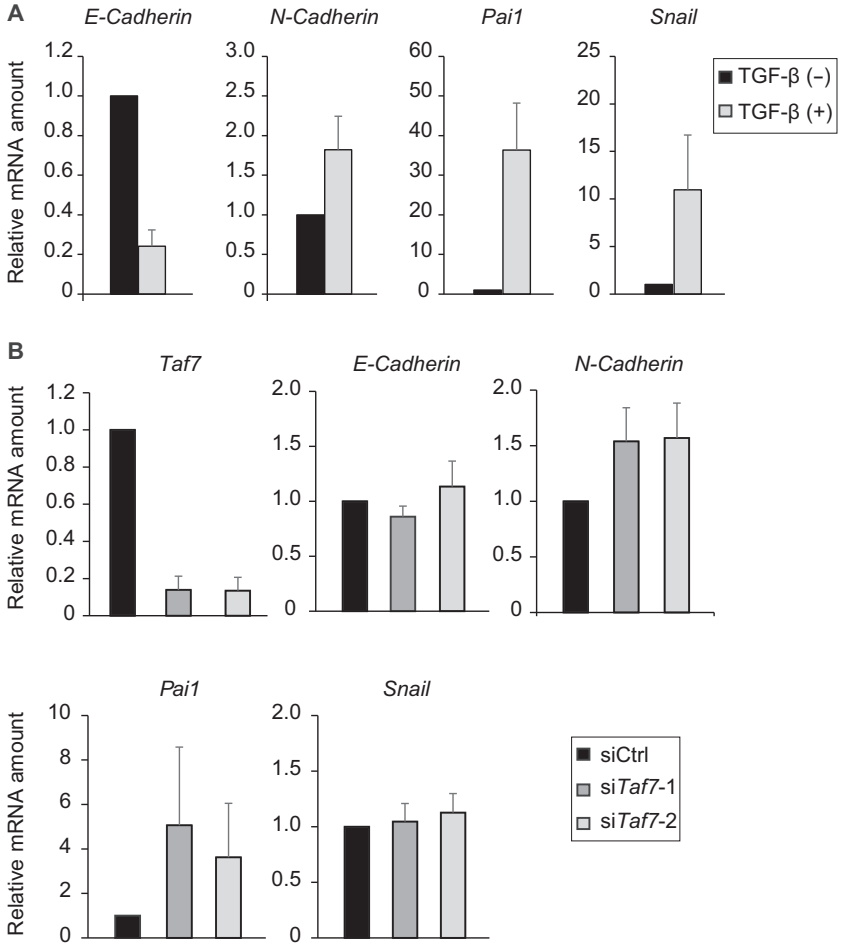

FIG 7 Knockdown of TAF7 does not induce EMT. (A) RT-qPCR analysis of EMT-related gene expression in NMuMG cells incubated in the absence or presence of TGF-β for 2 days. Data are means and SEM for three independent experiments. (B) RT-qPCR analysis of *Taf7* and EMT-related gene expression in NMuMG cells transfected with either of two siRNAs targeting *Taf7* mRNA or with a negative-control siRNA (siCtrl). Data are means and SEM for three independent experiments.

generated NMuMG cells that overexpressed MYC through retroviral infection (Fig. 10A). The expression of TRIM26 under both basal and TGF-β-stimulated conditions as well as the TGF-β-induced degradation of TAF7 was suppressed by MYC overexpression (Fig. 10A and B). Overexpressed MYC remained associated with the SBE1 region of the *Trim26* promoter even in the presence of TGF-β, and the TGF-β-induced binding of SMAD3 to SBE1 and SBE2 was suppressed in the MYC-overexpressing cells (Fig. 10C), supporting the notion that the association of MYC with the E-box adjacent to SBE1 interferes with SMAD3 recruitment to the *Trim26* promoter. Consistent with these observations, activation of the *Trim26* promoter by TGF-β was significantly attenuated by MYC overexpression (Fig. 10D), and this effect of MYC overexpression was prevented by deletion of the E-box (Fig. 10E). Furthermore, MYC overexpression attenuated the proliferative arrest induced by TGF-β to an extent similar to that observed after *Trim26* knockout (Fig. 5A and 10F). However, whereas TGF-β-induced apoptosis was attenuated by *Trim26* deletion (Fig. 6A), it was enhanced by MYC overexpression (Fig. 10G), possibly as a result of effects of MYC on proapoptotic target genes (30). Together these results suggest that MYC directly suppresses *Trim26* expression and thereby inhibits degradation of TAF7 and counteracts the antiproliferative function of TGF-β.

TGF-β-induced proliferative arrest mediated by TRIM26-dependent TAF7 degradation and its antagonism by MYC in RMT-1 E4 cells. To examine the generality of TRIM26 induction by TGF-β, we treated RMT-1 E4 rat mammary epithelial cells with

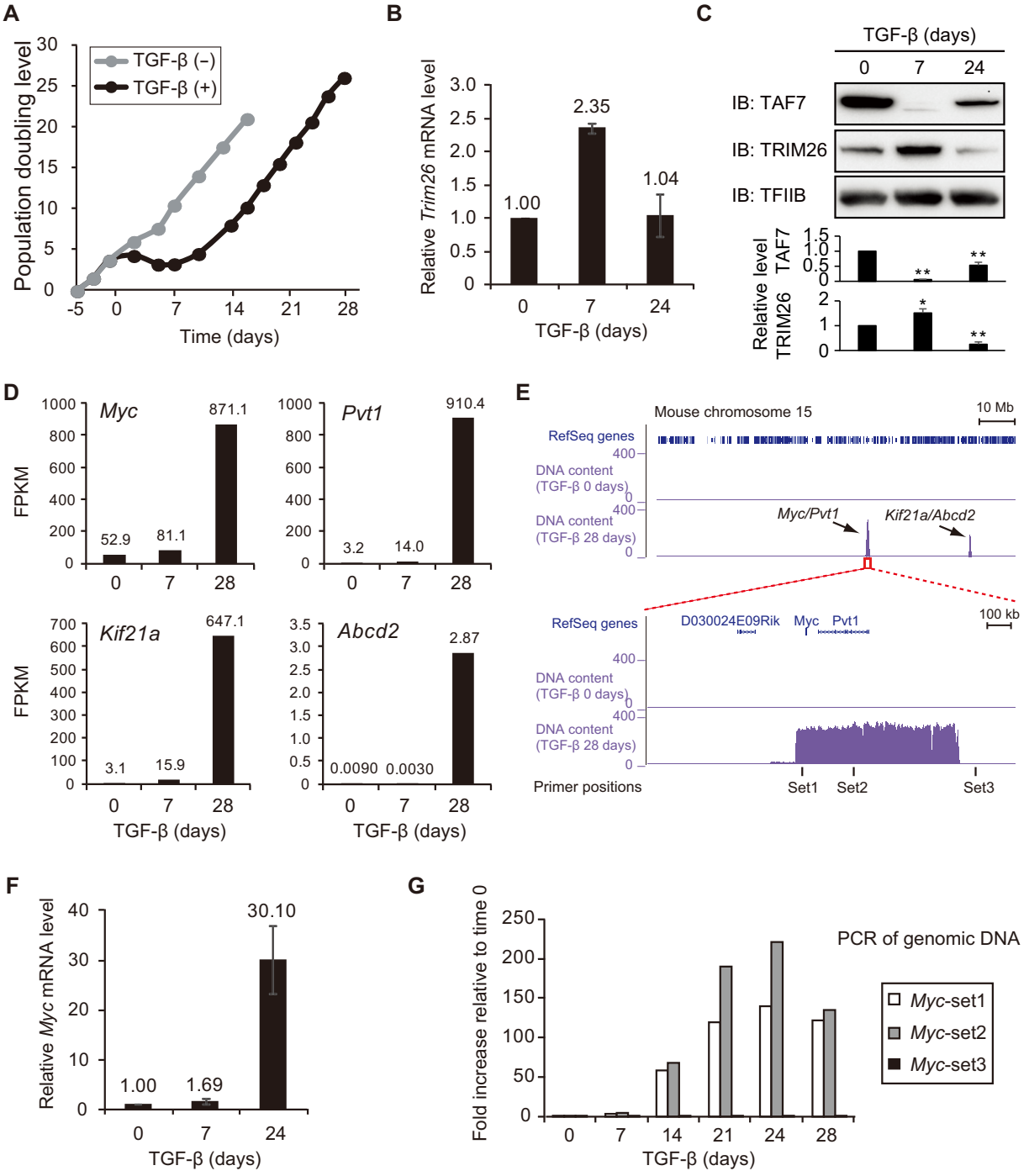

FIG 8 *Myc* amplification in NMuMG cells subjected to sustained TGF-β treatment. (A) Analysis of NMuMG cell proliferation during culture in the absence or presence of TGF-β. TGF-β was added at time zero. Data are from a representative experiment. (B) RT-qPCR analysis of *Trim26* mRNA in NMuMG cells treated with TGF-β for the indicated times. Data are means and SEM for two independent experiments. (C) Immunoblot analysis of TAF7, TRIM26, and TFIIB (loading control) in NMuMG cells incubated with TGF-β for the indicated times. The band intensities for TAF7 and TRIM26 normalized to those for TFIIB are shown as means and SEM for three independent experiments. *, $P < 0.05$; **, $P < 0.01$ (one-way ANOVA followed by Tukey's *post hoc* test). (D) RNA-seq analysis of the indicated genes in NMuMG cells treated with TGF-β for the indicated times. FPKM, fragments per kilobase of exon model per million mapped fragments. (E) Amplification of two genomic regions on chromosome 15 in NMuMG cells treated with TGF-β for 28 days is shown in the upper panel, and the boxed region containing *Myc* and *Pvt1* is shown enlarged in the lower panel. The positions of primers for the genomic PCR analysis in panel G are also indicated. (F) RT-qPCR analysis of *Myc* expression in NMuMG cells treated with TGF-β for the indicated times. Data are means $\pm$ SEM for two independent experiments. (G) Genomic PCR analysis of DNA content around the *Myc/Pvt1* locus with the primer sets shown in panel E for NMuMG cells treated with TGF-β for the indicated times. DNA samples were independent of those used for panel E.

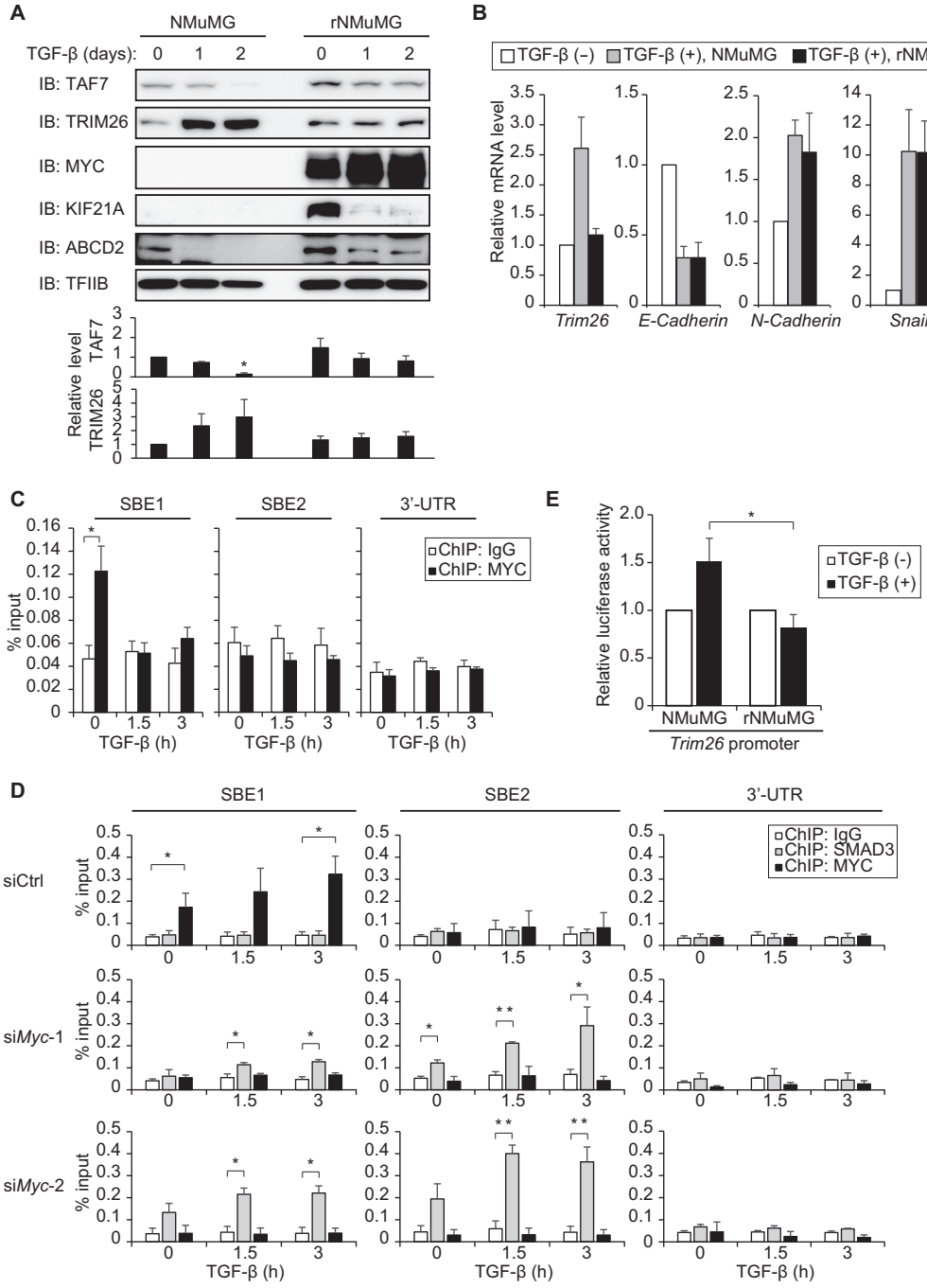

FIG 9 rNMuMG cells are resistant to TRIM26 induction by TGF-β. (A) Immunoblot analysis of the indicated test proteins and TFIIB (loading control) in parental NMuMG cells and rNMuMG cells incubated with TGF-β for the indicated times. The band intensities for TAF7 and TRIM26 normalized to those for TFIIB are shown as means and SEM for three independent experiments. *, $P < 0.05$ versus corresponding time zero (two-way ANOVA followed by Tukey's *post hoc* test). (B) RT-qPCR analysis of *Trim26* and EMT-related gene expression in parental NMuMG cells and rNMuMG cells incubated in the absence or presence of TGF-β for 2 days. Data are means and SEM for three independent experiments. (C) ChIP-qPCR analysis of the binding of MYC to the *Trim26* promoter region. NMuMG cells exposed to TGF-β for the indicated times were fixed, lysed, and subjected to ultrasonic treatment followed by ChIP with antibodies to MYC or control IgG. Precipitated DNA was quantified by qPCR with primers specific for the indicated regions of *Trim26*. Data are means and SEM for three independent experiments. *, $P < 0.05$ (two-way ANOVA followed by Tukey's *post hoc* test). (D) ChIP-qPCR analysis of SMAD3 and MYC binding to the *Trim26* promoter region in rNMuMG cells transfected with either of two *Myc* siRNAs or a control siRNA and then treated with TGF-β for the indicated times. Data are means and SEM for three independent experiments. *, $P < 0.05$; **, $P < 0.01$ (two-way ANOVA followed by Tukey's *post hoc* test). (E) Luciferase reporter assay of *Trim26* promoter activity in parental NMuMG cells and rNMuMG cells treated (or not) with TGF-β for 24 h. Data are means and SEM for four independent experiments. *, $P < 0.05$ (two-way ANOVA followed by Tukey's *post hoc* test).

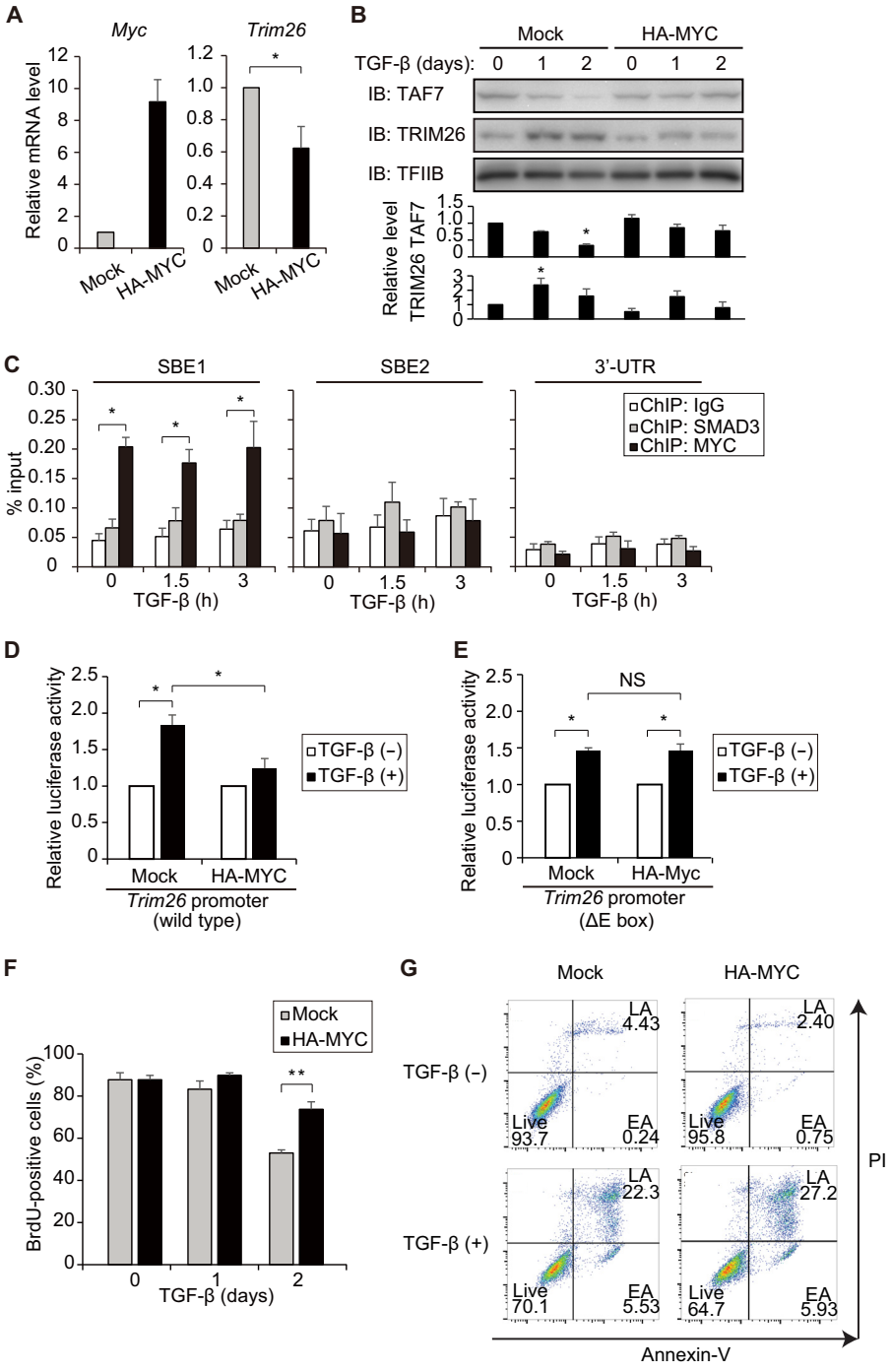

FIG 10 MYC suppresses TRIM26 induction by TGF-β. (A) RT-qPCR analysis of *Myc* and *Trim26* expression in NMuMG cells stably infected with a retrovirus encoding HA-MYC or with the corresponding empty virus as a control (mock). Data are means and SEM for three independent experiments. *, $P < 0.05$ (unpaired Student's *t* test). (B) Immunoblot analysis of TAF7, TRIM26, and TFIIB (loading control) in control and HA-MYC-expressing NMuMG cells treated with TGF-β for the indicated times. The band intensities for TAF7 and TRIM26 normalized to those for TFIIB are shown as means and SEM for three independent experiments. *, $P < 0.05$ versus corresponding time zero (two-way ANOVA followed by Tukey's *post hoc* test). (C) ChIP-qPCR analysis of SMAD3 and MYC binding to the *Trim26* promoter region in HA-MYC-expressing NMuMG cells exposed to TGF-β for the indicated times. Data are means and SEM for three independent experiments. *, $P < 0.05$ (two-way ANOVA followed by Tukey's *post hoc* test). (D) Luciferase reporter assay of *Trim26* promoter activity in HA-MYC-expressing or control NMuMG cells treated (or not) with TGF-β for 24 h. Data are means and SEM for four independent experiments. *, $P < 0.05$ (two-way ANOVA followed by Tukey's *post hoc* test). (E) Luciferase reporter assay of the activity of a mutant form of the *Trim26* promoter lacking the E-box (ΔE box) in HA-MYC-expressing or control NMuMG cells treated (or not) with TGF-β for 24 h. Data are means and SEM for four independent experiments. *, $P < 0.05$

(Continued on next page)

TGF-β and found that it elicited TRIM26 expression and loss of TAF7 as well as proliferation arrest and apoptosis (data not shown). Thus, targeting of TRIM26 by TGF-β is not restricted to NMuMG cells but rather occurs in mammary epithelial cells of both the mouse and rat. We also generated RMT-1 E4 cells that overexpressed MYC through retroviral infection to test whether MYC overexpression suppressed TRIM26 induction in these cells. The induction of TRIM26 by TGF-β as well as the TGF-β-induced degradation of TAF7 was suppressed by MYC overexpression (data not shown). Furthermore, MYC overexpression attenuated the proliferative arrest induced by TGF-β in RMT-1 E4 cells, although it enhanced TGF-β-induced apoptosis as evaluated by immunoblot analysis of cleaved caspase-3 (data not shown), similar to its effect in NMuMG cells (Fig. 10G). Together these results indicate that the TGF-β–TRIM26–TAF7 axis and its antagonism by MYC overexpression are not restricted to mouse cells but are conserved in rat mammary epithelial cells.

DISCUSSION

Cellular differentiation processes have been found to be associated with the downregulation of various TFIID components mediated by transcriptional repression. Proteasomal degradation has also been implicated in such downregulation of TBP and TAF4a in differentiating C2C12 myoblasts and F9 embryonal carcinoma cells (12), with HUWE1 recently identified as a ubiquitin ligase that targets TBP for degradation (13). We have now identified TRIM26 as a ubiquitin ligase that targets the TFIID component TAF7 for proteasomal degradation, suggesting that posttranslational regulation of TFIID subunits may be widespread. Why is the abundance of TFIID components regulated by both transcriptional and posttranslational mechanisms? Given that we found that TGF-β induces both proteasomal degradation of TAF7 and upregulation of *Taf7* mRNA, cessation of proteasomal degradation is likely followed by a rapid recovery of TAF7 levels after termination of TGF-β stimulation. Characterization of the mechanism by which TRIM26 is inactivated after TGF-β withdrawal should provide further insight into such regulation.

TRIM26 is a RING finger-type ubiquitin ligase with three previously identified substrates. TRIM26 thus binds to and ubiquitylates IRF3 for proteasomal degradation in the nucleus in response to interferon stimulation (31). Similar to the effect of TGF-β described in the present study, interferon stimulation upregulates TRIM26 expression, indicating that TRIM26 is a stimulus-activated ubiquitin ligase. TRIM26 also ubiquitylates PHF20 and thereby triggers its degradation in the nucleus in a manner dependent on its recruitment by the histone demethylase JMJD3, serving as a scaffold protein (32). In addition, the DNA base excision repair-related DNA glycosylase NEIL1 was recently identified as a substrate for TRIM26-dependent degradation, with suppression of *Trim26* expression resulting in the accumulation of NEIL1 and increased resistance to ionizing radiation (33). Given that IRF3, PHF20, and TAF7 are all involved in gene transcription and NEIL1 is involved in DNA repair, it is likely that TRIM26 is an important regulator of gene transcription and repair in response to cellular stimulation. Furthermore, the recent finding that TRIM26 serves as a tumor suppressor of hepatocellular carcinoma (34) is consistent with our finding that TRIM26 functions as a negative regulator of cell proliferation by targeting TAF7 for degradation. Although our results support the notion that TAF7 is the major substrate of TRIM26 in the induction of proliferation arrest and apoptosis by TGF-β, we do not exclude the possibility that other TRIM26 substrates (IRF3, PHF20, NEIL1, or as yet unidentified proteins) also contribute to these effects.

FIG 10 Legend (Continued)
(two-way ANOVA followed by Tukey's *post hoc* test); NS, not significant. (F) HA-MYC-expressing or control NMuMG cells treated with TGF-β for the indicated times were assayed for BrdU incorporation by immunostaining. Data are means and SEM for four independent experiments. **, $P < 0.01$ (two-way ANOVA followed by Tukey's *post hoc* test). (G) HA-MYC-expressing or control NMuMG cells incubated in the absence or presence of TGF-β for 2 days were stained with PI and annexin V for flow cytometric analysis of apoptosis.

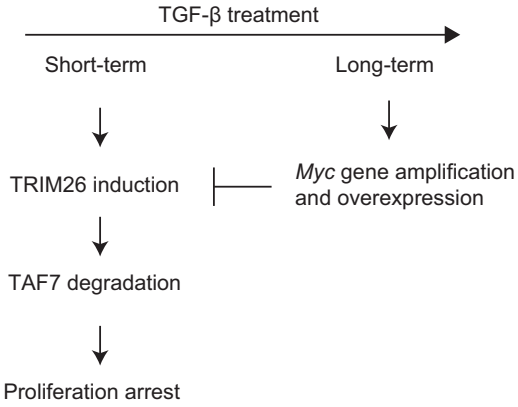

FIG 11 Proposed model for regulation of cell proliferation by TGF-β. Short-term treatment with TGF-β induces expression of the TRIM26 ubiquitin ligase, which ubiquitylates TAF7 for proteasomal degradation and thereby arrests cell proliferation. In contrast, long-term treatment with TGF-β results in amplification of the *Myc* gene, with consequent overexpression of MYC repressing TRIM26 induction and thereby allowing resumption of cell proliferation.

Downregulation of MYC mRNA by TGF-β has previously been shown to be important for proliferation arrest in epithelial cells (15, 35). However, we did not detect such an effect of TGF-β in NMuMG cells (data not shown), suggesting that transcriptional repression of the MYC gene by TGF-β is cell type specific. In this regard, it will be interesting to determine whether cells depleted of MYC are able to overcome the antiproliferative effect of TGF-β during long-term exposure to the cytokine.

Our data indicate that overexpressed MYC competes with SMAD3 for binding to the *Trim26* promoter and thereby inhibits *Trim26* expression. Given that MYC binds to the *Trim26* promoter, we propose that MYC directly regulates *Trim26* expression (Fig. 11). However, we do not exclude the possibility that transcriptional repressors induced by MYC also contribute to this regulation, as a global transcription amplifier model for MYC posits (36). How MYC competes with SMAD3 at target genes requires clarification in order to provide further insight into the molecular mechanisms of transcriptional repression by MYC.

TGF-β has been known to induce characteristics of malignant tumors in precancerous cells, with concomitant inhibition of proliferation (3, 4), but how this negative effect on proliferation is overcome in cancer cells has remained poorly understood. The *Myc* gene is frequently amplified in aggressive tumors (14), and the abundance of MYC mRNA or protein has been found to correlate with the rate of cell proliferation (15, 16). Genome-wide analysis has shown that MYC regulates the expression of various genes, many of which are related to the cell cycle (15). Our findings now connect TGF-β and MYC at the level of a shared target gene, *Trim26*, with TGF-β signaling inducing and MYC suppressing *Trim26* expression. Such regulation has opposite outcomes with regard to cell proliferation, with MYC counteracting the antiproliferative activity of TGF-β in a manner independent of the EMT process.

We detected amplification of two genomic regions on the same chromosome, accompanied by an upregulation of transcript abundance for four genes within these regions, in proliferating NMuMG cells after sustained exposure to TGF-β. Although *Myc* amplification likely contributes to this proliferative phenotype, we cannot exclude the possibility that the other three genes (*Pvt1*, *Kif21a*, and *Abcd2*) also play a role. Expression of PVT1 has been found to be required for upregulation of MYC protein levels in human cancer cells showing amplification of chromosome 8 (37). KIF21A is an inhibitor of microtubule growth (38), and its knockdown was shown to induce a lysosomal trafficking defect followed by lysosomal membrane disruption and consequent cell death (39), suggesting that *Kif21a* amplification might support cell survival by maintaining lysosomal trafficking. ABCD2 is a lipid transporter that mediates the import of very-long-chain fatty acids into the lumen of peroxisomes for β-oxidation

(40). Overexpression of ABCD2 might be expected to support cell proliferation through facilitation of energy production by β-oxidation or sequestration of excess very-long-chain fatty acids. Further studies are necessary to clarify the potential contributions of these three genes to cell proliferation during long-term exposure to TGF-β.

MATERIALS AND METHODS

Reagents. TGF-β1, MG132, and MLN4924 were obtained from R&D Systems, Peptide Institute, and Active Biochem, respectively.

Cell culture. NMuMG cells (CRL-1636; ATCC) were maintained in Dulbecco's modified Eagle's medium (DMEM) supplemented with 10% fetal bovine serum, penicillin (50 U/ml), streptomycin (50 μg/ml), 2 mM L-glutamine, 1% minimum essential medium (MEM)-nonessential amino acids, 1% sodium pyruvate, and insulin (8 μg/ml). 293T cells were maintained in the same medium without insulin. RMT-1 E4 cells (JCRB0242) were maintained in DMEM–F-12 GlutaMAX medium supplemented with 10% fetal bovine serum, penicillin (50 U/ml), and streptomycin (50 μg/ml). All cell lines were confirmed to be negative for mycoplasma contamination.

Cell counting. The population doubling level of cells was calculated by adding [log (cell number at passage) − log (cell number at previous passage)]/log (days during passage) at each passage.

Plasmid construction. Mammalian cell expression vectors were constructed by insertion of mouse cDNAs encoding TAF7, TRIM26, SMURF1, or RNF157 into the p3FLAG, pcDNA3-HA, or pcDNA3-myc vector. The pcDNA3-RNF19B-V5 vector was kindly provided by M. Kaneko (41). Mammalian knockout vectors were constructed as described previously (42). Bacterial expression vectors were constructed by insertion of mouse cDNAs encoding IκBα, TRIM26, or TAF7 into pGEX6P3 or mouse cDNAs for TRIM26 or UBCH5 isoforms into pET30a. E2 enzyme expression vectors were kindly provided by K. I. Nakayama. Retroviral expression vectors were constructed by insertion of mouse cDNAs encoding TAF7-3×FLAG, hemagglutinin (HA)- or EGFP-TRIM26, or HA-MYC into the pMX-puro or pMX-blast vector. Retroviral vectors for shRNAs were constructed by insertion of the target sequences indicated in the figure legends into the pSR-puro vector.

siRNAs. Small interfering RNAs targeting mouse *Taf7* (s76882 and s202747) as well as a negative-control siRNA (medium GC) were obtained from Thermo Fisher Scientific. Those targeting mouse *Myc* were described previously (43).

Retrovirus infection. Retroviruses were produced in Plat-E cells (44) and were applied to target cells in the presence of Polybrene (1 μg/ml). The infected cells were selected by culture with puromycin (2.5 μg/ml).

RNA isolation and RT-qPCR analysis. RNA was isolated by use of an SV Total RNA isolation system (Promega) and subjected to RT with a PrimeScript RT reagent kit (TaKaRa Bio) followed by real-time PCR analysis with a StepOnePlus real-time PCR system (Life Technologies) and Fast SYBR green master mix (Life Technologies). Data were analyzed according to the $2^{-\Delta\Delta CT}$ method and were normalized to the amount of *Cul1* mRNA. The sequences of PCR primers are listed in Table S1 in the supplemental material.

Immunoprecipitation and immunoblot analyses. Immunoprecipitation and immunoblot analyses were performed as described previously (45). Band intensities were measured with ImageJ software. Antibodies used are listed in Table S2.

Luciferase reporter assay. The mouse *Trim26* promoter region spanning nucleotides −421 to +427 relative to the transcription start site was amplified by PCR, and four tandem copies of the promoter region were ligated into the pGL4.12 luciferase reporter vector (Promega) to yield pGL4.12-Trim26. The SBE deletion mutants of pGL4.12-Trim26 were constructed by PCR-based mutagenesis. Luciferase activities were measured by use of a Dual-Luciferase reporter assay system (Promega). The ratio of firefly to *Renilla* luciferase activity was calculated.

ChIP-qPCR. ChIP was performed as described previously (46). Primer sequences for ChIP-qPCR are listed in Table S1.

Analysis of microarray data. Public microarray data (CEL files) were obtained from the NCBI Gene Expression Omnibus (GEO) (accession number GSE44050). The expression values of the CEL files were normalized with the justRMA function in the affy package of R/Bioconductor (https://www.bioconductor.org), in which the CDF environment is "MO_GENE10ST_MM_REFSEQ." The resultant normalized expression values were averaged and used to calculate the fold changes in expression levels for NMuMG cells treated with TGF-β for 2 days relative to those for untreated cells.

DNA-seq and RNA-seq. DNA-seq and RNA-seq libraries were prepared by use of an Ovation Ultralow DR multiplex system (NuGEN) and a TruSeq Standard mRNA LT sample prep kit (Illumina), respectively. All libraries were clonally amplified in the flow cell of an Illumina HiSeq 2500 instrument and sequenced (51-nucleotide paired-end sequencing). Paired-end reads from RNA-seq were mapped to the mouse genome (UCSC mm9 and RefSeq) by use of TopHat (ver. 2.0.8) (47). Cufflinks (ver. 2.0.10) was used to estimate gene expression levels on the basis of fragments per kilobase of exon model per million mapped fragments (FPKM) (48). The mapped reads of DNA were converted to BigWig format for visualization of DNA content throughout the genome in the UCSC genome browser. Primer sequences for genomic DNA quantification was as follows: set1-F, 5′-TTCGCTACTGCTGAATGTGG-3′; set1-R, 5′-TAACCCTCCAGGCATCAAAG-3′; set2-F, 5′-AAGCAGGGGAGATGTCATTG-3′; set2-R, 5′-ACACCAATTTGAGCCAGGAC-3′; set3-F, 5′-CACATGGGCAGACATCAATC-3′; and set3-R, 5′-ATGACCCCAGAAGTGAATGC-3′.

Ubiquitylation assays. Ubiquitylation assays were performed as described previously (45).

BrdU incorporation assay. Cells treated with 10 μM BrdU for 24 h were fixed with 4% paraformaldehyde, permeabilized with 0.5% Triton X-100 in phosphate-buffered saline (PBS), denatured with 2 M

HCl, washed with PBS containing 0.1% Tween 20 (PBS-T), and exposed to 1% bovine serum albumin in PBS before incubation with antibodies to BrdU (Table S2). The cells were then washed with PBS-T, incubated with Alexa Fluor 555-labeled secondary antibodies (Thermo Fisher Scientific), washed again with PBS-T, treated with 4′,6-diamidino-2-phenylindole (DAPI; 1 μg/ml), and examined with a BZ-9000 microscope (Keyence).

Flow cytometry. Flow cytometry was performed as previously described (49).

Statistical analysis. Quantitative data are presented as means ± standard errors of the means (SEM) and were evaluated with Student's *t* test or by one-way or two-way analysis of variance (ANOVA) followed by Tukey's *post hoc* test, with the sample size having been determined to allow such analysis. *P* values of <0.05 were considered to be statistically significant.

Accession number(s). Raw FASTQ files from the present study have been deposited in the DDBJ Sequence Read Archive (DRA) database under accession number DRA004089.

SUPPLEMENTAL MATERIAL

Supplemental material for this article may be found at https://doi.org/10.1128/MCB.00449-17.

SUPPLEMENTAL FILE 1, PDF file, 0.1 MB.

ACKNOWLEDGMENTS

We thank T. Kitamura for pMX-puro and Plat-E cells, M. Kaneko for pcDNA3-RNF19B-V5, K. I. Nakayama for E2 expression vectors, H. Takahashi for sharing unpublished data and for discussions, Y. Nagasawa for technical assistance, T. Konishi for secretarial assistance, other laboratory members for discussions, and the Biomedical Research Core of the Tohoku University Graduate School of Medicine for technical support.

This work was funded by KAKENHI grants 25891003 and 17K14955 to T.N., 15K18453 to M.H., 26830064 to R.F., and 26293059, 15K15024, and 17H04035 to K.N. from the Japan Society for the Promotion of Science.

We declare that we have no conflicts of interest.

REFERENCES

1. Shi Y, Massague J. 2003. Mechanisms of TGF-β signaling from cell membrane to the nucleus. Cell 113:685–700. https://doi.org/10.1016/S0092-8674(03)00432-X.
2. Hanahan D, Weinberg RA. 2011. Hallmarks of cancer: the next generation. Cell 144:646–674. https://doi.org/10.1016/j.cell.2011.02.013.
3. Miyazono K. 2009. Transforming growth factor-β signaling in epithelial-mesenchymal transition and progression of cancer. Proc Jpn Acad Ser B Phys Biol Sci 85:314–323. https://doi.org/10.2183/pjab.85.314.
4. Pardali K, Moustakas A. 2007. Actions of TGF-β as tumor suppressor and pro-metastatic factor in human cancer. Biochim Biophys Acta 1775:21–62.
5. Thomas MC, Chiang CM. 2006. The general transcription machinery and general cofactors. Crit Rev Biochem Mol Biol 41:105–178. https://doi.org/10.1080/10409230600648736.
6. Naar AM, Lemon BD, Tjian R. 2001. Transcriptional coactivator complexes. Annu Rev Biochem 70:475–501. https://doi.org/10.1146/annurev.biochem.70.1.475.
7. Goodrich JA, Tjian R. 2010. Unexpected roles for core promoter recognition factors in cell-type-specific transcription and gene regulation. Nat Rev Genet 11:549–558. https://doi.org/10.1038/ni0710-549.
8. Nakayama KI, Nakayama K. 2006. Ubiquitin ligases: cell-cycle control and cancer. Nat Rev Cancer 6:369–381. https://doi.org/10.1038/nrc1881.
9. Nakagawa T, Nakayama K. 2015. Protein monoubiquitylation: targets and diverse functions. Genes Cells 20:543–562. https://doi.org/10.1111/gtc.12250.
10. Deshaies RJ, Joazeiro CA. 2009. RING domain E3 ubiquitin ligases. Annu Rev Biochem 78:399–434. https://doi.org/10.1146/annurev.biochem.78.101807.093809.
11. Rotin D, Kumar S. 2009. Physiological functions of the HECT family of ubiquitin ligases. Nat Rev Mol Cell Biol 10:398–409. https://doi.org/10.1038/nrm2690.
12. Perletti L, Kopf E, Carre L, Davidson I. 2001. Coordinate regulation of RARγ2, TBP, and TAFII135 by targeted proteolysis during retinoic acid-induced differentiation of F9 embryonal carcinoma cells. BMC Mol Biol 2:4. https://doi.org/10.1186/1471-2199-2-4.
13. Li L, Martinez SS, Hu W, Liu Z, Tjian R. 2015. A specific E3 ligase/deubiquitinase pair modulates TBP protein levels during muscle differentiation. Elife 4:e08536. https://doi.org/10.7554/eLife.08536.
14. Beroukhim R, Mermel CH, Porter D, Wei G, Raychaudhuri S, Donovan J, Barretina J, Boehm JS, Dobson J, Urashima M, Mc Henry KT, Pinchback RM, Ligon AH, Cho YJ, Haery L, Greulich H, Reich M, Winckler W, Lawrence MS, Weir BA, Tanaka KE, Chiang DY, Bass AJ, Loo A, Hoffman C, Prensner J, Liefeld T, Gao Q, Yecies D, Signoretti S, Maher E, Kaye FJ, Sasaki H, Tepper JE, Fletcher JA, Tabernero J, Baselga J, Tsao MS, Demichelis F, Rubin MA, Janne PA, Daly MJ, Nucera C, Levine RL, Ebert BL, Gabriel S, Rustgi AK, Antonescu CR, Ladanyi M, Letai A, Garraway LA, Loda M, Beer DG, True LD, Okamoto A, Pomeroy SL, Singer S, Golub TR, Lander ES, Getz G, Sellers WR, Meyerson M. 2010. The landscape of somatic copy-number alteration across human cancers. Nature 463:899–905. https://doi.org/10.1038/nature08822.
15. Dang CV. 2012. MYC on the path to cancer. Cell 149:22–35. https://doi.org/10.1016/j.cell.2012.03.003.
16. Kress TR, Sabo A, Amati B. 2015. MYC: connecting selective transcriptional control to global RNA production. Nat Rev Cancer 15:593–607. https://doi.org/10.1038/nrc3984.
17. Lin CY, Lovén J, Rahl PB, Paranal RM, Burge CB, Bradner JE, Lee TI, Young RA. 2012. Transcriptional amplification in tumor cells with elevated c-Myc. Cell 151:56–67. https://doi.org/10.1016/j.cell.2012.08.026.
18. Nie Z, Hu G, Wei G, Cui K, Yamane A, Resch W, Wang R, Green DR, Tessarollo L, Casellas R, Zhao K, Levens D. 2012. c-Myc is a universal amplifier of expressed genes in lymphocytes and embryonic stem cells. Cell 151:68–79. https://doi.org/10.1016/j.cell.2012.08.033.
19. Sabò A, Kress TR, Pelizzola M, de Pretis S, Gorski MM, Tesi A, Morelli MJ, Bora P, Doni M, Verrecchia A, Tonelli C, Fagà G, Bianchi V, Ronchi A, Low D, Müller H, Guccione E, Campaner S, Amati B. 2014. Selective transcriptional regulation by Myc in cellular growth control and lymphomagenesis. Nature 511:488–492. https://doi.org/10.1038/nature13537.
20. Walz S, Lorenzin F, Morton J, Wiese KE, von Eyss B, Herold S, Rycak L, Dumay-Odelot H, Karim S, Bartkuhn M, Roels F, Wüstefeld T, Fischer M, Teichmann M, Zender L, Wei CL, Sansom O, Wolf E, Eilers M. 2014. Activation and repression by oncogenic MYC shape tumour-specific

gene expression profiles. Nature 511:483–487. https://doi.org/10.1038/nature13473.
21. Meyer N, Penn LZ. 2008. Reflecting on 25 years with MYC. Nat Rev Cancer 8:976–990. https://doi.org/10.1038/nrc2231.
22. Wolf E, Lin CY, Eilers M, Levens DL. 2015. Taming of the beast: shaping Myc-dependent amplification. Trends Cell Biol 25:241–248. https://doi.org/10.1016/j.tcb.2014.10.006.
23. Miettinen PJ, Ebner R, Lopez AR, Derynck R. 1994. TGF-β induced transdifferentiation of mammary epithelial cells to mesenchymal cells: involvement of type I receptors. J Cell Biol 127:2021–2036. https://doi.org/10.1083/jcb.127.6.2021.
24. Tiwari N, Tiwari VK, Waldmeier L, Balwierz PJ, Arnold P, Pachkov M, Meyer-Schaller N, Schübeler D, van Nimwegen E, Christofori G. 2013. Sox4 is a master regulator of epithelial-mesenchymal transition by controlling Ezh2 expression and epigenetic reprogramming. Cancer Cell 23:768–783. https://doi.org/10.1016/j.ccr.2013.04.020.
25. Soucy TA, Smith PG, Milhollen MA, Berger AJ, Gavin JM, Adhikari S, Brownell JE, Burke KE, Cardin DP, Critchley S, Cullis CA, Doucette A, Garnsey JJ, Gaulin JL, Gershman RE, Lublinsky AR, McDonald A, Mizutani H, Narayanan U, Olhava EJ, Peluso S, Rezaei M, Sintchak MD, Talreja T, Thomas MP, Traore T, Vyskocil S, Weatherhead GS, Yu J, Zhang J, Dick LR, Claiborne CF, Rolfe M, Bolen JB, Langston SP. 2009. An inhibitor of NEDD8-activating enzyme as a new approach to treat cancer. Nature 458:732–736. https://doi.org/10.1038/nature07884.
26. Massague J, Seoane J, Wotton D. 2005. Smad transcription factors. Genes Dev 19:2783–2810. https://doi.org/10.1101/gad.1350705.
27. Gegonne A, Tai X, Zhang J, Wu G, Zhu J, Yoshimoto A, Hanson J, Cultraro C, Chen QR, Guinter T, Yang Z, Hathcock K, Singer A, Rodriguez-Canales J, Tessarollo L, Mackem S, Meerzaman D, Buetow K, Singer DS. 2012. The general transcription factor TAF7 is essential for embryonic development but not essential for the survival or differentiation of mature T cells. Mol Cell Biol 32:1984–1997. https://doi.org/10.1128/MCB.06305-11.
28. Gal A, Sjoblom T, Fedorova L, Imreh S, Beug H, Moustakas A. 2008. Sustained TGF β exposure suppresses Smad and non-Smad signalling in mammary epithelial cells, leading to EMT and inhibition of growth arrest and apoptosis. Oncogene 27:1218–1230. https://doi.org/10.1038/sj.onc.1210741.
29. Xu J, Chen Y, Olopade OI. 2010. MYC and breast cancer. Genes Cancer 1:629–640. https://doi.org/10.1177/1947601910378691.
30. Hoffman B, Liebermann DA. 2008. Apoptotic signaling by c-MYC. Oncogene 27:6462–6472. https://doi.org/10.1038/onc.2008.312.
31. Wang P, Zhao W, Zhao K, Zhang L, Gao C. 2015. TRIM26 negatively regulates interferon-β production and antiviral response through polyubiquitination and degradation of nuclear IRF3. PLoS Pathog 11:e1004726. https://doi.org/10.1371/journal.ppat.1004726.
32. Zhao W, Li Q, Ayers S, Gu Y, Shi Z, Zhu Q, Chen Y, Wang HY, Wang RF. 2013. Jmjd3 inhibits reprogramming by upregulating expression of INK4a/Arf and targeting PHF20 for ubiquitination. Cell 152:1037–1050. https://doi.org/10.1016/j.cell.2013.02.006.
33. Edmonds MJ, Carter RJ, Nickson CM, Williams SC, Parsons JL. 2017. Ubiquitylation-dependent regulation of NEIL1 by Mule and TRIM26 is required for the cellular DNA damage response. Nucleic Acids Res 45:726–738. https://doi.org/10.1093/nar/gkw959.
34. Wang Y, He D, Yang L, Wen B, Dai J, Zhang Q, Kang J, He W, Ding Q, He D. 2015. TRIM26 functions as a novel tumor suppressor of hepatocellular carcinoma and its downregulation contributes to worse prognosis. Biochem Biophys Res Commun 463:458–465. https://doi.org/10.1016/j.bbrc.2015.05.117.
35. Massague J. 2008. TGFβ in cancer. Cell 134:215–230. https://doi.org/10.1016/j.cell.2008.07.001.
36. Rahl PB, Young RA. 2014. MYC and transcription elongation. Cold Spring Harb Perspect Med 4:a020990. https://doi.org/10.1101/cshperspect.a020990.
37. Tseng YY, Moriarity BS, Gong W, Akiyama R, Tiwari A, Kawakami H, Ronning P, Reuland B, Guenther K, Beadnell TC, Essig J, Otto GM, O'Sullivan MG, Largaespada DA, Schwertfeger KL, Marahrens Y, Kawakami Y, Bagchi A. 2014. PVT1 dependence in cancer with MYC copy-number increase. Nature 512:82–86. https://doi.org/10.1038/nature13311.
38. van der Vaart B, van Riel WE, Doodhi H, Kevenaar JT, Katrukha EA, Gumy L, Bouchet BP, Grigoriev I, Spangler SA, Yu KL, Wulf PS, Wu J, Lansbergen G, van Battum EY, Pasterkamp RJ, Mimori-Kiyosue Y, Demmers J, Olieric N, Maly IV, Hoogenraad CC, Akhmanova A. 2013. CFEOM1-associated kinesin KIF21A is a cortical microtubule growth inhibitor. Dev Cell 27:145–160. https://doi.org/10.1016/j.devcel.2013.09.010.
39. Groth-Pedersen L, Aits S, Corcelle-Termeau E, Petersen NH, Nylandsted J, Jaattela M. 2012. Identification of cytoskeleton-associated proteins essential for lysosomal stability and survival of human cancer cells. PLoS One 7:e45381. https://doi.org/10.1371/journal.pone.0045381.
40. Morita M, Imanaka T. 2012. Peroxisomal ABC transporters: structure, function and role in disease. Biochim Biophys Acta 1822:1387–1396. https://doi.org/10.1016/j.bbadis.2012.02.009.
41. Kaneko M, Iwase I, Yamasaki Y, Takai T, Wu Y, Kanemoto S, Matsuhisa K, Asada R, Okuma Y, Watanabe T, Imaizumi K, Nomura Y. 2016. Genome-wide identification and gene expression profiling of ubiquitin ligases for endoplasmic reticulum protein degradation. Sci Rep 6:30955. https://doi.org/10.1038/srep30955.
42. Ran FA, Hsu PD, Wright J, Agarwala V, Scott DA, Zhang F. 2013. Genome engineering using the CRISPR-Cas9 system. Nat Protoc 8:2281–2308. https://doi.org/10.1038/nprot.2013.143.
43. Ishikawa Y, Hosogane M, Okuyama R, Aoyama S, Onoyama I, Nakayama KI, Nakayama K. 2013. Opposing functions of Fbxw7 in keratinocyte growth, differentiation and skin tumorigenesis mediated through negative regulation of c-Myc and Notch. Oncogene 32:1921–1932. https://doi.org/10.1038/onc.2012.213.
44. Morita S, Kojima T, Kitamura T. 2000. Plat-E: an efficient and stable system for transient packaging of retroviruses. Gene Ther 7:1063–1066. https://doi.org/10.1038/sj.gt.3301206.
45. Nakagawa T, Araki T, Nakagawa M, Hirao A, Unno M, Nakayama K. 2015. S6 kinase- and β-TrCP2-dependent degradation of p19Arf is required for cell proliferation. Mol Cell Biol 35:3517–3527. https://doi.org/10.1128/MCB.00343-15.
46. Hosogane M, Funayama R, Shirota M, Nakayama K. 2016. Lack of transcription triggers H3K27me3 accumulation in the gene body. Cell Rep 16:696–706. https://doi.org/10.1016/j.celrep.2016.06.034.
47. Trapnell C, Pachter L, Salzberg SL. 2009. TopHat: discovering splice junctions with RNA-Seq. Bioinformatics 25:1105–1111. https://doi.org/10.1093/bioinformatics/btp120.
48. Trapnell C, Hendrickson DG, Sauvageau M, Goff L, Rinn JL, Pachter L. 2013. Differential analysis of gene regulation at transcript resolution with RNA-seq. Nat Biotechnol 31:46–53. https://doi.org/10.1038/nbt.2450.
49. Funayama R, Taniguchi H, Mizuma M, Fujishima F, Kobayashi M, Ohnuma S, Unno M, Nakayama K. 2017. Protein-arginine deiminase 2 suppresses proliferation of colon cancer cells through protein citrullination. Cancer Sci 108:713–718. https://doi.org/10.1111/cas.13179.